Fractal Growth Phenomena

Tamás Vicsek

Institute for Technical Physics
Budapest, Hungary

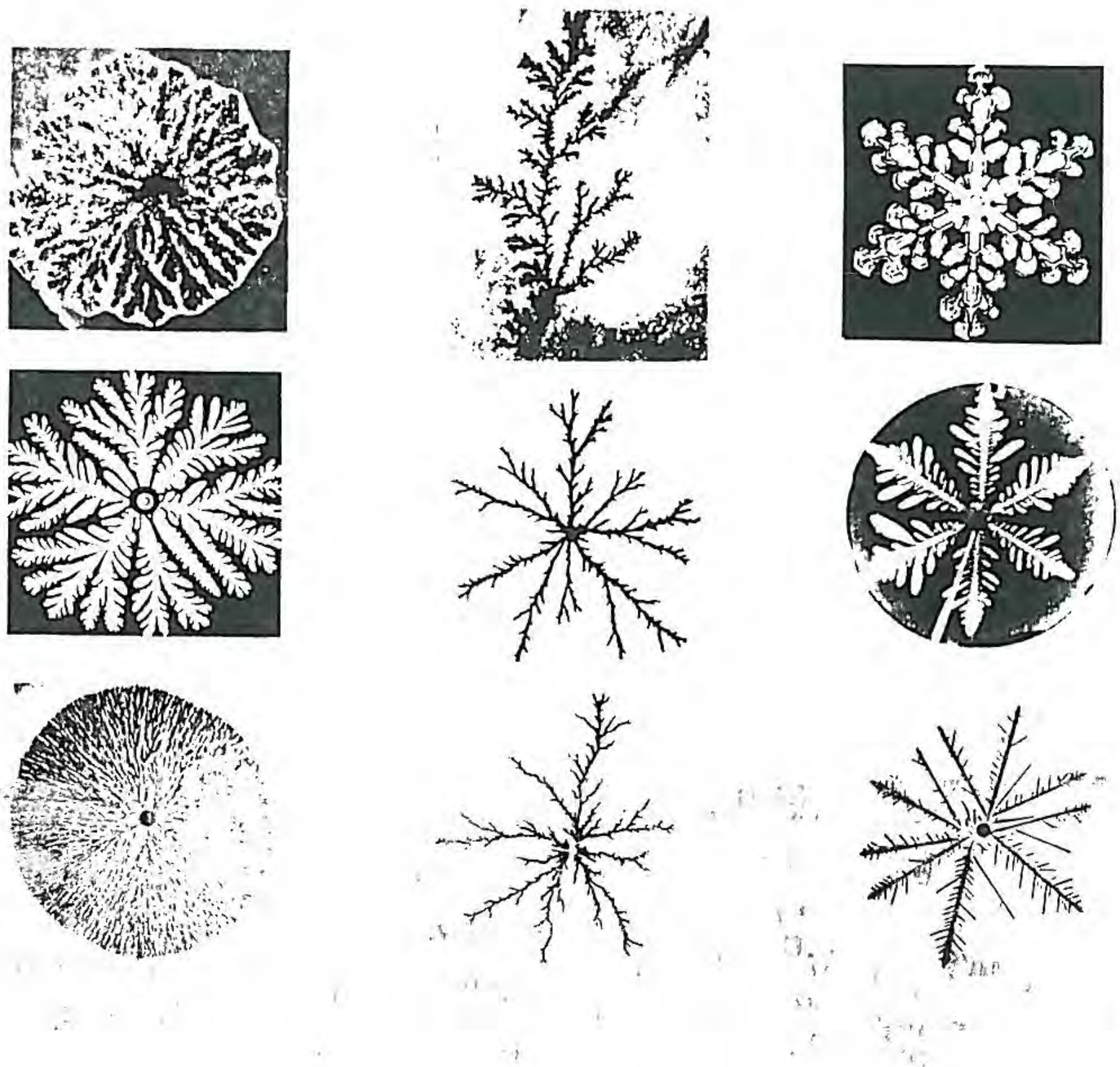

WORLD SCIENTIFIC
Singapore

$D = A \cdot b^{\alpha}$

/

Scaling, $C(r) \sim A r^{\alpha}$ $r \to br$ $C(br) \sim D r^{\alpha}$
new - analitikus, kritikus viselkedés, kritikus pont
universális kritikus exponenser

PART I.

FRACTALS

Chapter 4.

METHODS FOR DETERMINING FRACTAL DIMENSIONS

When one tries to determine the fractal dimension of growing structures in practice, it usually turns out that the direct application of definitions for D given in the previous two chapters is ineffective or can not be accomplished. Instead, one is led to measure or calculate quantities which can be shown to be related to the fractal dimension of the objects.

Three main approaches are used for the determination of these quantities: experimental, computer and theoretical. *Experiments* represent a standard way of examining phenomena in every field of physics and they have been playing an important role in the development of research concerning fractal growth as well. The situation is less typical in the case of the other two approaches. Since the physics of fractal growth lacks a unified theoretical description, most of the investigations prompted by theoretical motivations are based on *computer simulation.* The only *theoretical* principle which seems to be applicable to a relatively wide range of growth processes is renormalization which will be discussed in the last Section following a discussion of the experimental and numerical methods for determining D.

4.1. MEASURING FRACTAL DIMENSIONS IN EXPERIMENTS

A number of experimental techniques have been used to measure the fractal dimension of scale invariant structures grown in various experiments. The most widely applied methods can be divided into the following categories: (a) digital image processing of two-dimensional pictures, (b) scattering experiments, (c) covering the structures with monolayers, and (d) direct measurement of dimension-dependent physical properties.

(a) *Digitizing the image* of a fractal object is a standard way of obtaining quantitative data about geometrical shapes. The information is picked up by a scanner or an ordinary video camera and transmitted into the memory of a computer (typically a PC). The data are stored in the form of a two-dimensional array of pixels whose non-zero (equal to zero) elements correspond to regions occupied (not occupied) by the image. Once they are in the computer, the data can be evaluated using the methods described in the next Section, where calculation of D for computer generated clusters is discussed.

The only principal question related to processing of pictures arises if two-dimensional images of objects embedded into three dimensions are considered. In Section 2.3.1. it has already been mentioned that the fractal dimension of the projection of an object onto a $(d-m)$-dimensional plane is the same as its original fractal dimension, if $D < d-m$. Unfortunately, there are only heuristic arguments supporting this assumption, and considerable deviations may occur from it, especially when D is only a bit smaller than $d-m$. In addition, if $D > d-m$ the method breaks down completely, since in this case the projection is simply a $(d-m)$-dimensional object.

(b) *Scattering experiments* represent a powerful method to measure the fractal dimension of microscopic structures (Teixeira 1986). Depending on the characteristic length scales associated with the object to be studied, light, X-ray or neutron scattering can be used to reveal fractal properties. There are a number of possibilities to carry out a scattering experiment. One can investigate i) the structure factor of a single fractal object, ii) scattering by many clusters growing in time, iii) the scattered beam from a fractal

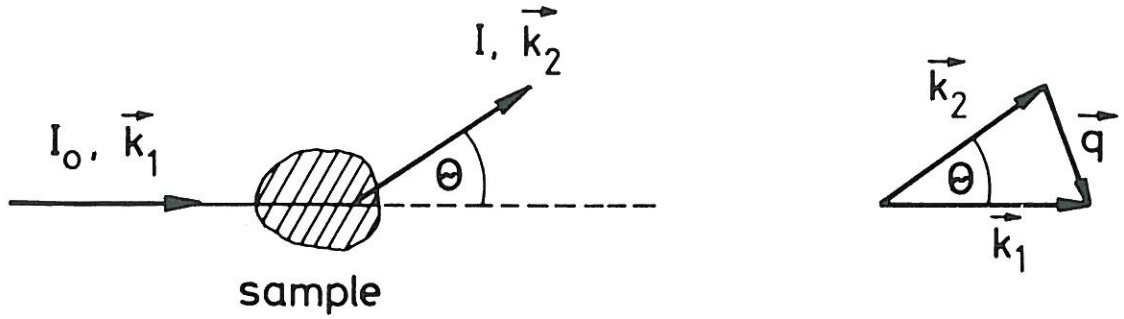

Figure 4.1. Schematic representation of the incident and scattered beams in a scattering experiment.

surface, etc.

In scattering experiments a beam of intensity I_0 is directed on the sample and the scattered intensity is measured as the function of the angle θ between the incident and the scattered beam. Let us denote the difference between the wave vectors corresponding to these beams denoted by $\vec{q} = \vec{k}_1 - \vec{k}_2$ (Fig. 4.1). In the case of small θ (small angle scattering) the main contribution to the scattered intensity comes from quasi-elastic processes with $|\vec{k}_1| = |\vec{k}| = k = 2\pi/\lambda$, where λ is the wavelength of the incident beam. Therefore, from Fig. 4.1

$$q = |\vec{q}| = 2k \sin(\theta/2). \tag{4.1}$$

Most of the fractal structures studied experimentally are made of small spherical particles whose size exceeds the spatial resolution typical in small angle X-ray (SAXS) or neutron (SANS) scattering experiments. Thus, it is useful to identify a single scatterer with a corresponding form factor $P(q)$ and separate the scattered intensity into two factors

$$I(q) = \rho_0 P(q)[1 + S(q)], \tag{4.2}$$

where ρ_0 is the average density in the sample, $S(q)$ is the interparticle structure factor and we assume that the particles are spherical having a radius r_0. It can be shown that for $qr_0 \ll 1$ the form factor is approximately constant

(Guinier regime), while for $qr_0 \gg 1$, $P(q) \sim q^{-4}$ which is called the Porod law.

According to the theory of scattering (see e.g. Squires 1978), the structure factor $S(q)$ is the Fourier transform of the density-density correlation function $c(r)$ defined by the expression (2.14). In a three dimensional isotropic system this means that

$$S(q) = 4\pi \int_0^\infty c(r) r^2 \frac{\sin(qr)}{qr} dr. \tag{4.3}$$

To calculate the actual shape of $S(q)$ we recall that for fractals the density correlations decay with a power law depending on D in the form $c(r) \sim r^{D-d}$ (See Eqs. (2.16) and (2.18)). For a finite object of average radius R, $c(r)$ is expected to decrease very quickly to zero for $r > R$ which, for $d = 3$, can be taken into account by the assumption

$$c(r) \sim r^{D-3} f(r/R), \tag{4.4}$$

where $f(x) \simeq$ constant for $x \ll 1$ and $f(x) \ll 1$ if $x \gg 1$. The cutoff function $f(x)$ is presumed to depend only on the ratio r/R because of the self-similar nature of the structure. Inserting (4.4) into (4.3) and changing the variable of integration $r = z/q$ we get

$$S(q) \sim q^{-D} \int_0^\infty z^{D-2} f(z/qR) \sin z dz. \tag{4.5}$$

This expression is expected to be valid in the range $qR \gg 1$ and $qr_0 \ll 1$, when the scattered beam probes the density correlations of particles within the object. Since in this case $f(x)$ is approximately constant up to large values of z, the integral in (4.5) only weakly depends on q and we can conclude that

$$I(q) \simeq S(q) \sim q^{-D} \qquad \text{for} \quad 1/R \ll q \ll 1/r_0, \tag{4.6}$$

since in this regime $P(q)$ is close to a constant. This is a result often used

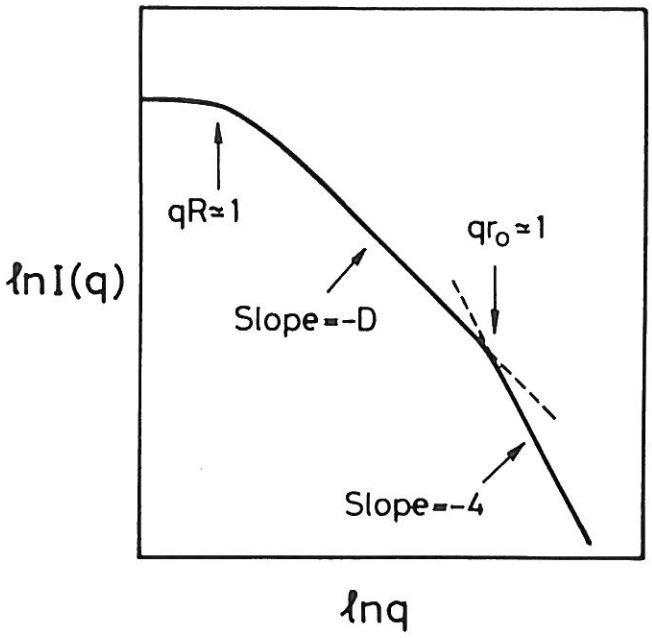

Figure 4.2. Schematic scattering curve showing the three main regimes which can be observed for an ensemble of fractal aggregates.

to estimate the fractal dimension of an experimental object. The statement that the integral in (4.5) is only weakly dependent on q can be supported by further calculations based on an assumption concerning the actual form of $f(x)$. Supposing that $f(r/R) \sim e^{-r/aR}$, where a is a constant, one can integrate (4.5) explicitly and arrive at (4.6) if $aqR \gg 1$.

Thus, in scattering experiments one can distinguish three major regimes (Fig. 4.2):

i) $qr_0 \gg 1 \gg qb$,

where b denotes the interatomic distance. In this case one probes the shape of the individual particles the structure is made of. This regime is characterized by a simple power law decay $I(q) \sim q^{-4}$ (Porod's law).

ii) $qR \gg 1 \gg qr_0$

This is the region of q values where (4.6) is expected to describe the spatial fluctuations of particles on a length scale smaller than the average radius of the object, R. In this case the fractal dimension can be determined from the slope of $\ln I(r)$ against $\ln q$.

iii) $1 \geq qR$

In this limit the fractal object behaves as a single particle from the point of view of small angle scattering. If a sufficiently dilute solution of clusters is present in the system, this regime allows the applicaton of an independent method for the determination of D which will be briefly discussed below.

According to the standard theory of scattering (Squires 1978), in the region corresponding to case iii) the structure factor can be approximated by the expresssion

$$S(q) \sim \frac{\rho_0 M_w}{(1 + q^2 R_z^2/3 + ...)}, \tag{4.7}$$

where $M_w = S(0)$ is the weight average molecular weight of the clusters and R_z is a quantity proportional to the average radius of the the clusters (it is equal to the so called z average radius of gyration). One expects that there is a relation between M_w and R_z (Schaefer *et al* 1984)

$$M_w \sim R_z^D \tag{4.8}$$

analogous to (2.2). Then one can determine D measuring $S(q)$ in a diluted system of aggregates *growing in time.* Because of (4.7) the intercept of $S(q)$ with the $q = 0$ axis provides M_w, while $S(q)$ starts to bend downward at $qR_z \simeq 1$. D can be obtained by making a log-log plot of these quantitites as a function of time.

The above analysis was concerned mainly with stochastic structures. It can be shown that light diffraction on deterministic fractals embedded into two dimensions results in a self-similar diffraction pattern (Allain and Cloitre 1986). In the related experiment a laser beam is directed onto the sample which is a structure obtained after a few steps of one of the deterministic constructions discussed in Section 2.3.1. The diffraction pattern observed on a screen represents an optical Fourier transform of the object. The corresponding structure factor $S(p, q)$ can also be calculated and its value averaged over the frequency bands scales according to (4.6). In particular, the optical diffraction pattern of the fractal shown in Fig. 2.1. and its calculated structure factor were found to be self-similar. This is demonstrated by Fig.4.3.

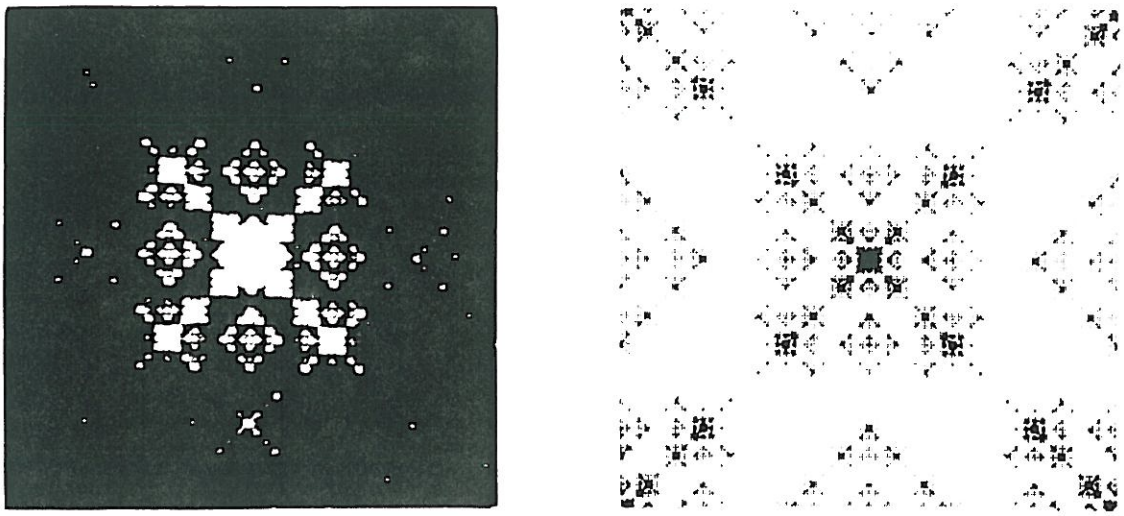

Figure 4.3. Optical diffraction pattern and the corresponding calculated structure factor of the fractal shown in Fig. 2.1a (k=5) (Allain and Cloitre 1986).

(c) To measure fractal dimensions by *covering the structure* with probe particles of varied radii (e.g. Pfeifer and Avnir 1983) is an obvious idea which is directly related to the definitions of D discussed in Chapter 2. In order to carry out an investigation of this sort one has to find materials which are well absorbed by the surface of the objects. In addition, the difference $\epsilon_{max} - \epsilon_{min}$ between the smallest and largest radii of the molecules has to be large enough so that at least two or three decades could be covered by the method. The fractal dimension is then obtained from the relation $n(\epsilon) \sim \epsilon^{-D}$ equivalent to (2.4), where $n(\epsilon)$ moles/g is the number of absorbent molecules forming a monolayer on the surface. This method is limited to measuring surface properties, since closed but empty regions inside a fractal object are not acccessible to the molecules. Obviously, the monolayer technique would give $D = 1$ for the Sierpinski gasket (Section 2.3.1.), provided we were confined to two dimensions, while the mathematical definition allows covering the fractal everywhere. On the other hand, it is expected to work well for open branching structures and surfaces.

In a simple variation of this method the size of the molecules is kept

constant and R, the radius of the particles having a fractal surface, is increased. In this case $n(\epsilon) \sim R^{D-3}$, where it is assumed that the number of particles/g scales as R^{-3}, i.e., they are not volume fractals.

Several experiments are based on the determination of the *cumulative volume* $V(r > \epsilon)$ of empty regions or holes with a characteristic radius larger than ϵ. A typical measurement of this type is used to study the structure of porous media. For example, in porositometry, mercury is injected into the object with a given capillary pressure p. The non-wetting mercury can only enter pores with a radius larger than the radius of curvature inversely proportional to p. The pore size distribution which can be related to the fractal dimension is then obtained from the change of the volume of injected mercury as a function of the increased pressure.

To find the ϵ dependence of $V(r > \epsilon)$ one can use the following heuristic argument (Pfeifer 1986). Let us cover the fractal structure with a minimum number $N(\epsilon)$ of balls of radius ϵ. Then the volume covered by the balls is

$$V(\epsilon) \sim N(\epsilon)\epsilon^3 \sim \epsilon^{3-D} \tag{4.9}$$

This is the volume which is is not available for particles (invading fluid) having a larger radius (radius of curvature) than ϵ, since by definition we do not cover empty regions with radius a larger than ϵ. Obviously, with decreasing ϵ, $V(\epsilon)$ decreases by an amount equal to the increase of $V(r > \epsilon)$, i.e., $-dV(\epsilon)/d\epsilon = dV(r > \epsilon)/d\epsilon$. From here

$$\frac{dV(r > \epsilon)}{d\epsilon} \sim -\epsilon^{2-D}, \tag{4.10}$$

where the left hand side can be determined experimentally for various ϵ and the corresponding log-log plots allow the calculation of D. Expression (4.10) corresponds to a rule mentioned in Section 2.3.1. according to which the number of holes of radius larger than ϵ usually scales as ϵ^{-D}.

When one uses a wetting fluid to cover a fractal (this might be especially useful in the case of macroscopic objects) the situation is similar

because the capillary forces lead to a characteristic curvature in such experiments as well (see Section 10.4). However, the geometry is inversed: Empty regions with a radius larger than that of the meniscus are not filled. Nevertheless, one expects that the volume of the wetting fluid surrounding the object depends on the radius of curvature ϵ according to the same law as above, namely, $V \sim \epsilon^{3-D}$ for a range of ϵ values (de Gennes 1985).

(d) Measurements of *physical properties* of fractal objects can also be used for the experimental determination of D. A number of methods have been suggested, most of them based on electrical properties including measurements of current, electromagnetic power dissipation and frequency dependence of the complex impedance of fractal interfaces. These methods typically provide an indirect estimate of D and have been used less extensively than the above discussed approaches.

4.2. EVALUATION OF NUMERICAL DATA

Throughout this Section we assume that the information about the stochastic structures is stored in the form of d-dimensional arrays which correspond to the values of a function given at the nodes (or sites) of some underlying lattice. In the case of studying geometrical scaling only, the value of the function attributed to a point with given coordinates (the point being defined through the indexes of the array) is either 1 (the point belongs to the fractal) or 0 (the site is empty). When multifractal properties are investigated the site function takes on arbritrary values. In general, such discrete sets of numbers are obtained by two main methods: i) by digitizing pictures taken from objects produced in experiments, ii) by numerical procedures used for simulation of various growth phenomena.

In the case of random growth numerically generated data are typically produced by variations of the Monte Carlo method. In addition, exact enumeration techniques and numerical integration of the corresponding equations can also be used. In Sec. 4.1. we discussed a number of techniques one can use to get information from an experimentally grown structure. Analogously, there are many ways of determining the fractal dimension D from

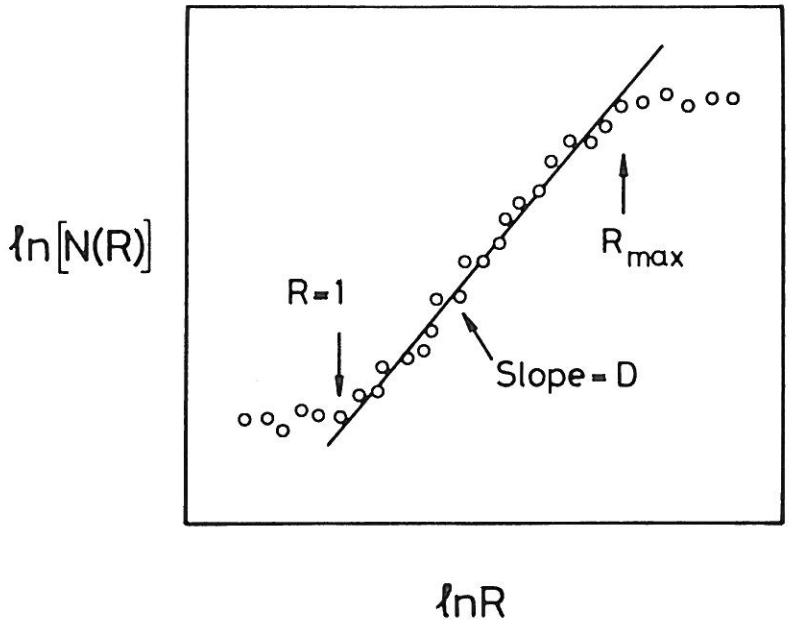

Figure 4.4. Schematic log-log plot of the numerically determined number of particles $N(R)$ belonging to a fractal and being within a sphere of radius R. If R is smaller than the particle size or larger than the linear size of the structure a trivial behaviour is observed. The fractal dimension is obtained by fitting a straight line to the data in the scaling region.

numerical data. Below we discuss how to measure D for a single object. To make the estimates more accurate one usually calculates the fractal dimension for *many clusters* and averages over the results.

Perhaps the simplest method is to use the definition of D as given in (2.2) and (2.3). In our case the unit length corresponds to the lattice constant, and the number of balls of unit volume $N(R)$ needed to cover the structure within a sphere of radius R is the same as the number of sites with a site function equal to 1 in the sphere. Since for growing fractals $N(R) \sim R^D$, plotting $\ln N(R)$ versus $\ln R$ results in a curve which has an asymptotic slope equal to D. (Strictly speaking $N(R) \sim R^D$ is valid only if there is an equivalence between the scaling observed by covering the structure with a lattice of boxes (box counting) and using boxes of increasing size centred on the same point (sandbox method). This equivalence exists only for uniform fractals with no multifractal spectrum of their "mass" distribution (see Section 3.4.))

Thus, the fractal dimension can be obtained by fitting a straight line to the asymptotic part of the $N(R)$ data, e.g., using the method of least squares. In practice one chooses a point belonging to the fractal (usually close to its centre of mass) and counts the number of sites belonging to the object within a sequence of spheres of growing radius. Instead of spheres one can also use boxes of linear size L. Fig. 4.4 shows a schematic plot of this kind demonstrating the crossovers which take place when R becomes smaller than the lattice constant and R is larger than the size of the structure.

If the fractal object consists of small, nearly identical particles, one can think of $N(R)$ as the number of particles within a region of volume R^d, i.e., $N(R) \sim M(R)$, where $M(R)$ is the mass of the cluster of radius R. For convenience, in the following we shall frequently use the terminology "particle" for a lattice site which belongs to the fractal (is filled) and cluster for the objects made of connected particles.

A variation of the above method is generally used if the total number of particles within a cluster is recorded during the growth. Such a situation is common for example in Monte Carlo simulations, where the structure is typically grown by subsequent addition of particles to the object. In this approach one first calculates a quantity $R_g(N)$ called radius of gyration using the expression

$$R_g(N) = \left(\frac{1}{N} \sum_{i=1}^{N} r_i^2 \right)^{1/2}, \tag{4.11}$$

where r_i is the distance of the ith particle from the center of mass of the cluster and N is the total number of particles in the cluster at the given stage of the growth process. Then, it is assumed that

$$R_g(N) \sim N^{\nu}, \tag{4.12}$$

where $\nu = 1/D$. Therefore, $1/D$ can be obtained from the slope of the plot $\ln R_g$ as a function of $\ln N$. (4.12) corresponds to the assumptions that i) in the asymtotic regime R_g is linearly proportional to the total radius of the

cluster, ii) corrections due to the boundary effects can be neglected and iii) the structure is not a geometrical multifractal.

The fractal dimension of random structures can be also estimated from their *density-density correlation function* $c(r)$. According to its definition (2.14), $c(r)d^dr$ is the probability of finding a particle in the volume d^dr being at a distance r from a given particle. As was discussed in Section 2.3.1. $c(r) \sim r^{D-d}$ and this expression allows the determination of D from the corresponding log-log plot. When calculating $c(r)$ the following procedure is followed. One chooses a particle within the cluster and counts the number of particles which are within a spherical shell of radius r and width δr, where typically $\delta r \simeq 0.1r$. Then the same calculation is repeated for other particles and the result is normalized taking into account the number of centres and the volume of the shells used. In order to avoid undesirable effects caused by anomalous contributions appearing at the edge of the cluster one should not choose particles as centres close to the boundary region.

Calculation of the correlation function is obviously closely related to the previously mentioned methods. Counting the number of particles in shells corresponds to determining the derivative of $N(r)$. The most advantageous feature of calculating D by determining $c(r)$ is provided by the fact that using this method one averages over many points within a single cluster which is expected to improve the statistics.

Sometimes there is a large, slowly decaying *correction* to the simple power law behaviour of $N(R)$ or $c(r)$. This correction may have various origins and forms. For example, if the growth takes place along a *surface*, the presence of the surface usually has an effect on the overall behaviour of the quantities used for determining D. To extract the information concerning D one assumes a special functional dependence of the correction. Then, instead of fitting a straight line to the $N(R)$ data one fits a curve of the following form

$$N(R) \simeq AR^D[1 + f(R)], \tag{4.13}$$

where A is a constant and $f(R)$ is a function which is typically chosen to be

decaying as an exponential or a power law (or a combination of these).

Selecting the most appropriate variables when plotting the results is another effective way to obtain more accurate data. Many times there already exists a theoretical result or a good guess of other source for the value of the fractal dimension. In such cases it is the deviation from this value which can be a quantity of interest. A common procedure is to plot for example $\ln[N(R)/R_g^D]$ versus $\ln R$, where D_g is a guess for the fractal dimension. If the true D is approximately equal to D_g, the straight part of the plot is close to a horizontal line, and any deviation can be magnified.

In some cases it is not only the fractal dimension one has a hypothesis for, but the entire functional dependence of $N(R)$ or $c(r)$ on their variables. The finite size of the samples which are investigated necessarily leads to a cutoff in the behaviour of these quantities at R or r values comparable with the cluster size. Because of the self-similar nature of fractals the actual form of the cutoff also scales with the total number of particles in a cluster, and its scaling behaviour is characterized by the same fractal dimension as that of the radius. This fact can be expressed by the assumption that

$$c(r) \sim (rR)^{D-d} f(r/R), \tag{4.14}$$

where $R \sim N^{1/D}$ is the radius of the cluster consisting of N particles and $f(x)$ is a cutoff function with $f(x) \simeq Constant$ for $x \ll 1$ and $f(x) \ll 1$ (exponentially small) for $x \gg 1$. According to the scaling assumption (4.14), if a structure is stochastically self-similar, the data obtained for $c(r)$ for various values of N should collapse onto the same universal curve $f(x)$, when $\ln[(rR)^{(d-D)} c(r)]$ is plotted against $\ln(r/R)$ using the correct value for D. A plot of this type is displayed in Fig. 4.5. The scaling shown in Fig. 4.5b both provides a check of self-similarity and leads to a more reliable estimate of the fractal dimension (Meakin 1987) than that obtained by attempting to fit a straight line to the plot of $\ln c(r)$ versus $\ln r$ over an intermediate range of length scales.

In case of a *fractal measure* defined on a growing structure, there is a weight or probability attributed to each particle. The generalized dimensions

a

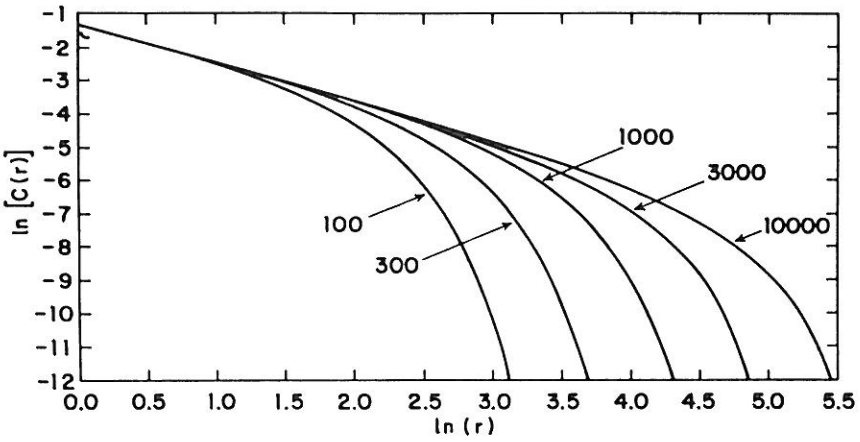

b

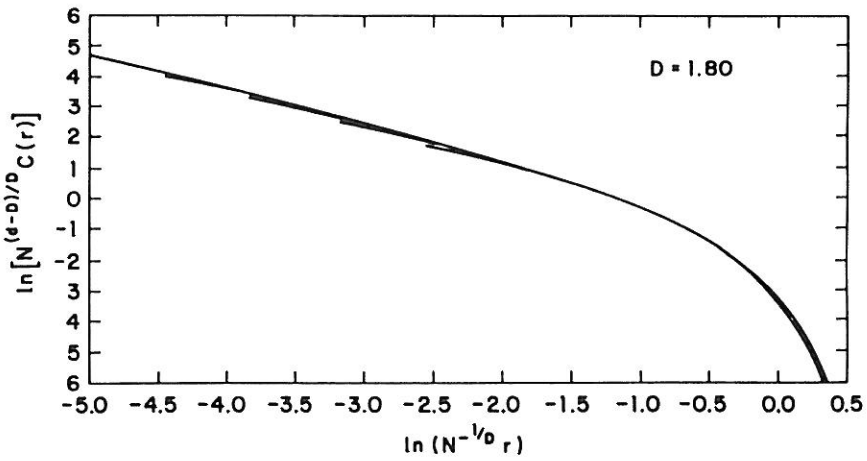

Figure 4.5. (a) Density-density correlation functions for three-dimensional off-lattice cluster-cluster aggregates (Section 8.1.1.). (b) Using the assumption (4.14) the data can be scaled onto a single curve (Meakin 1987).

D_q for such objects can be obtained using a procedure analogous to the box counting method described at the beginning of this Section. The only difference is that instead of simply counting the number of particles within a region of radius R, one calculates $\chi_q(R)$, the sum of the qth power of probabilities associated with the particles as a function of R. Then the generalized dimensions can be determined from the slopes of plots of $\ln \chi_q(R)$ versus $\ln R$, since according to (3.7) $\ln \chi_q(R) \sim (q-1)D_q \ln R$. The $f(\alpha)$ spectrum is obtained from D_q by Legendre transformation (see (3.11), (3.14) and (3.15)).

When discussing various evaluation techniques we assumed that the necessary data are already available. To obtain the arrays of coordinates corresponding to the positions of particles belonging to a fractal ususally requires numerical procedures depending on the particular physical process which is to be investigated. There are, however, a few general remarks which should be considered when one simulates the growth of fractals in a computer.

For example, when applying the flexible Monte Carlo method one typically adds particles to the growing cluster according to some rules given by the model which is used to simulate the phenomenon. The true fractal behaviour is manifested only for $N \to \infty$ while, obviously, a computer simulation has limitations concerning the total number of particles N. In case of slow crossovers between different kinds of scaling behaviour – which is typical for many growth phenomena – the data have to be extrapolated with special care. Taking into account correction-to-scaling terms (4.13) or finite size effects (4.14) are examples for such analysis. Another possibility is to use periodic boundary conditions when it is possible, and in this way mimic an infinite system by a periodic sequence of finite subsystems.

Finally, in stochastic simulations randomness is introduced with the help of *random number generators.* Here again, one has to be careful, because it can be easily shown that the simplest methods fail to produce a long sequence of staistically uncorrelated random numbers. This problem can be avoided by "mixing" two random number generators (Stauffer 1986).

Exact enumeration techniques provide an alternative to Monte Carlo methods to generate data for the determination of fractal dimensions. Here the philosophy is quite different; instead of generating large clusters with stochastic deviations from the true average behaviour, one studies small clusters exactly and extracts results from careful extrapolation to the large system limit. Growth phenomena are not very suitable for such approaches because in most of the models the same configuration can be realized in many ways each contributing to the average scaling with a different weight. This fact usually makes the calculations prohibitively expensive.

In the case of modelling growing self-avoiding walks (Sec. 5.4.2) the

situation is less complicated since there is a unique sequence leading to a given chain. For self-interacting growing walks each configuration of N steps (particles) has its own weight (probability) which is associated with it when calculating the average radius of the walks. Let us denote by $\langle R_e^2(N)\rangle$ the mean-square end-to-end distance and suppose that it is proportional the mean-squared radius of a chain. To obtain D from the enumeration data one assumes the following scaling form (Djordjevic *et al* 1983)

$$\langle R_e^2(N)\rangle = AN^{2/D}(1 + BN^{-\Delta} + CN^{-1} + ...), \tag{4.15}$$

where A, B and C are constants and Δ is a non-trivial correction-to-scaling exponent. (4.15) is expected to be a good approximation for $N \gg 1$. From the above expression one finds an estimate for the fractal dimension defined for clusters consisting of N particles

$$D(N) = 2\frac{\ln[(N+i)/N]}{\ln[\langle R_e^2(N+i)\rangle/\langle R_e^2(N)\rangle]} = D + \frac{\Delta B}{2}N^{-\Delta} + \frac{C}{2}N^{-1} + ... \tag{4.16}$$

Assuming that $\Delta > 1$ one finds D from the intercept of the plot of $D(N)$ against $1/N$ with the $D(N)$ axis at $1/N = 0$ (see Sec. 5.4.2). The value of the integer number i is usually chosen to be 1 or 2 depending on the type of lattice on which the growth takes place.

To complete the analysis it has to be shown that the correction-to-scaling exponent is indeed larger than unity. This can be done by plotting the quantity $\ln[D(N) - D]$ versus $\ln N$, where D is the asymptotic value as determined by the above extrapolation. If $\Delta > 1$, one gets a slope equal to -1; otherwise the slope is equal to $-\Delta$.

4.3. RENORMALIZATION GROUP

It has already been mentioned in the Introduction that there is a close relationship between fractals and critical phenomena. In the experiments on systems exhibiting second order phase transition a power law dependence of the relevant physical quantities was observed. The exponents characterizing

the scaling of these quantities were found to have non-integer values just like the mass of a growing fractal scales with its radius according to an exponent D which is not an integer number. In fact, the analogy is deep, since it is self-similarity which is behind non-standard scaling in both cases. This was shown in the investigations of critical phenomena where the scale invariance of the systems at the critical point was demonstrated by both experimental and theoretical approaches.

The above scale invariance forms the basis of renormalization group theory which has been successfully applied to the description of continuous phase transition through the calculation of the critical exponents and the so called phase diagrams revealing the relevance of the parameters effecting the transition. The idea of the Position-Space Renormalization Group (PSRG) approach is to renormalize a system with many degrees of freedom into a system having less degrees of freedom. The origin of many (infinite) degrees of freedom and scale invariance is the same: at the critical point the system possesses large fluctuations (regions belonging to one of the two phases) with no characteristic size.

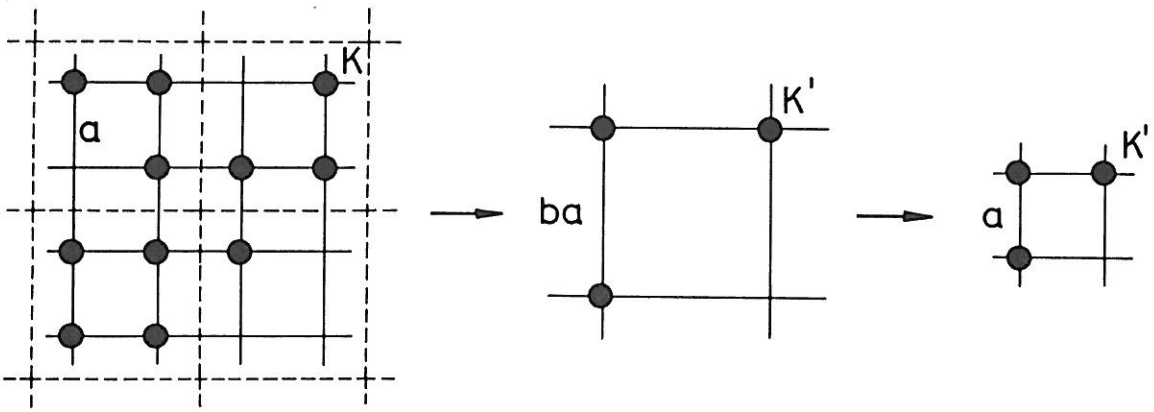

Figure 4.6. During this simple version of position-space renormalization four sites of the original system are replaced with a single new site having a renormalized fugacity K'. In this example the factor by which the linear size of the system is rescaled is equal to $b = 2$.

In the course of application of PSRG a part of the system defined on a lattice is replaced with a cell containing smaller number of sites (Fig. 4.6).

In order to account for scale invariance, however, during this transformation one has to change the weights associated with the filled sites so that the two systems (the original and the renormalized one) behave in the same way. The successive replacement of larger parts of the system with smaller ones is an *inverse analogue* of the recursive generation of deterministic fractals. At its critical point an infinite system is invariant under the renormalization procedure.

It is a quite obvious idea to try to apply this concept to growth phenomena leading to fractal structures. The renormalization scheme to be described below is analogous to the PSRG used for calculating critical exponents of equilibrium systems (Stanley *et al* 1982), and is based on the *generating function* (Nakanishi and Family 1985)

$$G(K) = \sum_{N=1}^{\infty} \sum_{i} P_{N,i} K^N, \tag{4.17}$$

where $P_{N,i}$ is the probability of creating the ith configuration consisting of N particles and K is a fugacity associated with each element of a cluster so that the total fugacity of a cluster is K^N. In the case of growth phenomena the total probability of generating clusters of size N is

$$\sum_{i} P_{N,i} = \sum_{i} \prod_{j=1}^{N} p_{N,i}(j) = 1, \tag{4.18}$$

since the creation of a cluster of N particles is a certain event (occurs with a probability equal to one) for all N, because of the ever growing character of the process. In the above expression $p_{N,i}(j)$ is the probability of adding the jth particle to the ith configuration of N particles. According to (4.18)

$$G(K) = \sum_{N=1}^{\infty} K^N. \tag{4.19}$$

This power series has a radius of convergence K_c=1.

Next we calculate R_g, the average radius of gyration of clusters using

the generating function (4.19). Since the radius of gyration of a cluster consisting of N particles scales as $R_g(N) \sim N^\nu$ with $\nu = 1/D$ (see preceding Section), we can determine the fractal dimension by finding a relation between $R_g(N)$ and N for a given growth process. The grand canonical average of $R_g(N)$ is

$$R_g = \frac{\sum_N N^\nu K^N}{\sum_N K^N} \sim (K_c - K)^{-\nu}. \tag{4.20}$$

To see this, one approximates the above sums by integrals (this can be done because the singular contribution to the sums come from the region $N \gg 1$). For the numerator one has

$$\begin{aligned} \int_0^\infty N^\nu K^N dN &\sim \int_0^\infty N^\nu e^{N \ln[1-(K_c-K)]}\, dN \\ &\sim (K_c - K)^{-\nu-1} \int_0^\infty z^\nu e^{-z} dz \sim (K_c - K)^{-\nu-1}, \end{aligned} \tag{4.21}$$

while similarly, the denominator in (4.20) diverges as $(K_c - K)^{-1}$. Therefore, if a quantity scales with growing N according to an exponent ν, the same quantity diverges with an exponent $-\nu$ when $K \to K_c = 1$. The calculation of D then reduces to the determination of ν for which the standard renormalization group method can be applied with the modifications discussed below.

As in usual critical phenomena the condition for renormalization is to *conserve a generalized form* of the generating function (4.17), while rescaling all lengths by a factor denoted by b. One should not consider the generating function (4.17) as a quantity to be conserved; this would always yield $K' = K$ and does not lead to any reasonable conclusion. Hypothetically exact renormalization would generate "further range interactions" which would require the consideration of many parameter generating functions and many-cell renormalization.

Instead, as a pragmatic simplification, one chooses a one-parameter formalism corresponding to a modified generating function based on the calculation of the most relevant contributions. This is achieved by equating the

renormalized fugacity K' to the contribution of spanning configurations to $G(K)$ within a cell of size b^d

$$K' = \sum_N \sum_{i'} P_{N,i'} K^N, \tag{4.22}$$

where $P_{N,i'}$ is given in (4.18). Here the second summation is quite non-trivial, it is taken over all spanning configurations (labelled by i') consisting of N particles, where spanning must be defined appropriately for each problem (Nakanishi and Family 1985).

From the known renormalization transformation $K'(K)$, the fractal dimension can be calculated by the usual fixed-point analysis. Let us linearize $K'(K)$

$$K_c - K' \simeq \lambda(K_c - K) \tag{4.23}$$

around its fixed point K_c, where $K'(K_c) = K_c$ and $\lambda = dK'/dK|_{K_c}$. On the other hand, R_g in the system with K is proportional to $(K_c - K)^{-\nu}$, while in the renormalized one $R_g \sim (K_c - K')^{-\nu}$. Since the system with fugacity K' is obtained by rescaling of the lattice units by a factor b, the condition that the radius of gyration should be invariant under the renormalization leads to

$$b(K_c - K')^{-\nu} \simeq (K_c - K)^{-\nu}. \tag{4.24}$$

Comparing (4.23) and (4.24) we find

$$D = \frac{1}{\nu} = \frac{\ln \lambda}{\ln b}, \tag{4.25}$$

where λ, the eingenvalue of the recursion relation (4.22) linearized around K_c can be calculated for small cells analytically, while for large cells it can be obtained using numerical methods.

To determine D in a small cell renormalization method one needs to calculate the sum of $P_{N,i}$-s corresponding to spanning configurations, where

the definition of spanning depends on the particular model to be renormalized. This will be demonstrated on the example of true self-avoiding walks at the end of this section. In general, small cell renormalization does not lead to good estimates for the fractal dimension in the case of growth models.

Large-cell Monte Carlo (MC) renormalization (Stanley *et al* 1982, Nakanishi and Family 1985) represents an alternative way to improve the accuracy without including more than one parameter. In this method cells with large b are considered, and the actual configurations are generated by a computer. Using larger cells is expected to lead to more reliable results for a number of reasons. Within a cell the behaviour of the system can be well approximated, and going to larger b increases the size of region which is treated with a good accuracy. In addition, undesirable surface effects are gradually eliminated as $b \to \infty$.

The basic idea is that the sum of $P_{N,i'}$-s taken over i' is nothing else than the fraction of spanning configurations of size N among all configurations consisting of N particles. Therefore, if we generate configurations randomly (according to the rules of the given model), then the sum of $P_{N,i'}$-s correspond to the fraction of spanning configurations among all the configurations generated. In this approach first one determines D_b, the fractal dimension obtained using cells of linear size b, and then plots these values against $1/\ln b$ to obtain the extrapolated value corresponding to the presumably exact $b \to \infty$ limit.

The Monte Carlo renormalization method can not be used with satisfactory results if the specific properties of clusters are disadvantageous with regard to the spanning rule. In the case of growth processes it is quite common that the behaviour of the clusters' surface is qualitatively different from their global properties. This fact is likely to be the reason for the unusually slow convergence of large-cell MC results.

The results can be improved by modifying the spanning rule. According to this modification, a cluster is considered as spanning the cell if its radius of gyration (R_g) becomes equal to $b/2$. R_g represents an averaging over the shape of the cluster and it is expected that the effects caused by

strong fluctuations in the surface structure can be eliminated by using R_g for characterizing the spatial extent of a cluster. A further improvement can be achieved by introducing a phenomenological parameter κ and assuming that κR_g should become equal to $b/2$. The "fixed point" κ^* of this optimization parameter is defined as the value for which the estimates of D for various b are the same. This method makes it possible to obtain accurate results using relatively small cells (see Section 6.1.3).

EXAMPLE

In this example we shall demonstrate how to apply small cell renormalization to cluster growth processes (Nakanishi and Family 1984), by calculating the fractal dimension of the so called true self-avoiding walks (TSAW-s). This is a simple, but inherently kinetic growth model with non-trivial behaviour different from that of ordinary random walks in dimensions not larger than two. A TSAW is a random walk which attempts to avoid itself whenever it is possible. In its simplest version treated here (more details about TSAW-s will be given in Section 5.4.1.) a true self-avoiding walk can cross itself only if there is no way to proceed without jumping into a site which already has been visited.

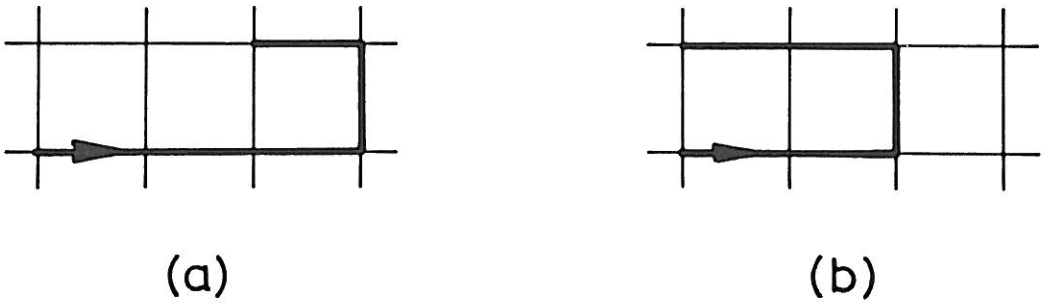

Figure 4.7. Two examples for true self-avoiding walks. Their weights are different, because the configuration 4.7b has two constrained steps, while 4.7a has only one (the last step).

By definition such a walk grows indefinitely and the statistics of a TSAW is controlled by its past history. This statement is illustrated by Fig.

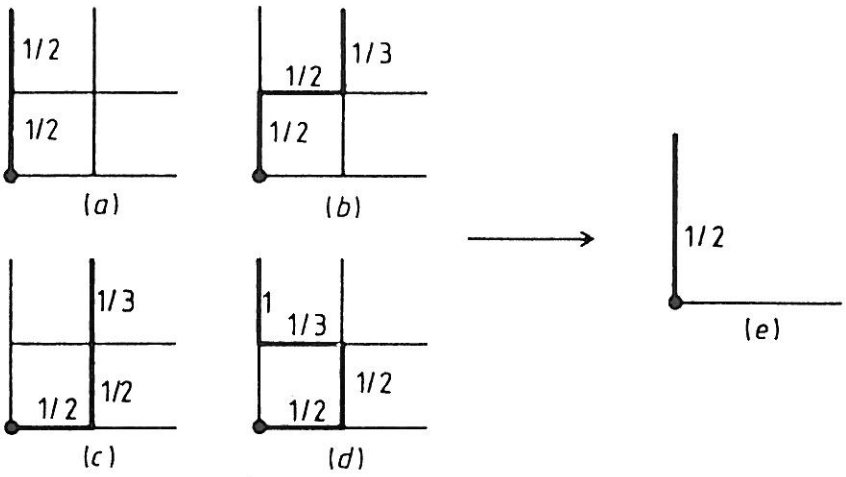

Figure 4.8. Spanning configurations of true self-avoiding walks in a 2×2 cell which are renormalized into one in (e). The probabilities corresponding to a given step are also indicated (Nakanishi and Family 1984).

4.7 showing two five steps walks. They are created with different probabilities $P_{5,1} = (\frac{1}{4})(\frac{1}{3})^3(\frac{1}{2})$ and $P_{5,2} = (\frac{1}{4})(\frac{1}{3})^2(\frac{1}{2})^2$, since the configuration Fig. 4.7b contains a constrained step at the end. Moreover, a walk has a different weight when traced in the opposite direction.

Application of the small cell renormalization approach on a 2×2 cell requires the calculation of the relative probability of spanning configurations. To make the spanning rule specific, we assume that all walks start at a corner site of the cell, and are restricted to stay within the cell until they exit via one of the external bonds. The probabilities $p_{N,i}(j)$ are calculated by counting at each step only those open bonds which are within the cell. Because of symmetry spanning in one direction is considered. Fig. 4.8 shows the spanning configurations together with their weights and the renormalized cell. According to this figure the renormalization transformation (4.22) for TSAW on a 2×2 cells has the form

$$\frac{1}{2}K' = \frac{1}{4}K^2 + \frac{1}{6}K^3 + \frac{1}{12}K^4. \tag{4.26}$$

From here $K_c = 1$ and $\lambda = dK'/dK|_{K_c} = \frac{8}{3}$. Using (4.25) yields for the fractal dimension $D = \ln(8/3)/\ln 2 \simeq 1.415$. The corresponding result for a 3×3

cell is somewhat larger, $D \simeq 1.419$. Calculations for the three dimensional case can be carried out analogously. For the $2 \times 2 \times 2$ cell one gets

$$\frac{1}{3}K' = \frac{1}{9}K^2 + \frac{1}{9}K^3 + \frac{11}{180}K^4 + \frac{29}{1080}K^5 + \frac{127}{8640}K^6 + \frac{79}{12960}K^7 + \frac{61}{25920}K^8 \tag{4.27}$$

which leads to $D \simeq 1.70$.

This example demonstrates the advantages and problems associated with small cell renormalization of growth models. The numerical results obtained are rather poor since it can be shown that the fractal dimension of TSAW is 2 for $d \geq 2$. On the other hand, small cell renormalization can provide qualitative information about D using simple algebra, even for highly non-trivial models. This method is more useful for studying growth processes depending on a parameter. Then, application of a two-parameter version of PSRG may reveal whether this parameter is relevant enough to change the fractal dimension. However, calculations of this sort published so far are based on approximations whose justification is not sufficiently satisfactory.

REFERENCES (PART I)

Allain, C. and Cloitre, M., 1986 *Phys. Rev.* **B33**, 3566

de Arcangelis, L., Redner, S. and Coniglio, A., 1985 *Phys. Rev.* **B31**, 4725

de Arcangelis, L., Redner, S. and Coniglio, A., 1986 *Phys. Rev.* **B34**, 4656

Besicovitch, A. S., 1935 *Mathematische Annalen* **110**, 321

Benzi, R., Paladin, G., Parisi, G. and Vulpiani, A., 1984 *J. Phys.* **A17**, 3521

Djordjevic, Z. V., Majid, I., Stanley, H. E. and dos Santos, 1983 *J. Phys.* **A16**, L519

Farmer, J. D., Ott, E. and Yorke, J. A., 1983 *Physica* **7D**, 153

Farmer, J. D., 1986 in *Dimensions and Entropies in Chaotic Systems* edited by E. Mayer-Kress (Springer, Berlin) p. 54

Frisch, U. and Parisi, G., 1984 in *Turbulence and Predictability in Geophysical*

Fluid Dynamics and Climate Dynamics, International School of Physics "Enrico Fermi", Course LXXXVIII, edited by M. Ghil, R. Benzi and G. Parisi (North-Holland, New York) p.84

de Gennes, P. G., 1985 in *Physics of Disordered Materials* edited by D. Adler, H. Fritzsche and S. R. Ovshinsky (Plenum Press, New York)

Halsey, T.C., Jensen, M. H., Kadanoff, L. P., Procacia, I. and Shraiman, B. I., 1986 *Phys. Rev.* **A33**, 1141

Hausdorff, F., 1919 *Mathhematische Annalen* **79**, 157

Hentschel, H. G. E. and Procaccia, I., 1983 *Physica* **8D**, 435

Kolmogorov, A. N. and Tihomirov, V. M., 1959 *Uspekhi Math. Nauk* **14**, 3

Mandelbrot, B. B., 1974 *J. Fluid. Mech.* **62**, 331

Mandelbrot, B. B., 1975 *Les Objects Fractals: Forme, Hasard et Dimension* (Flammarion, Paris)

Mandelbrot, B. B., 1977 *Fractals: Form, Chance and Dimension* (Freeman, San Francisco)

Mandelbrot, B. B., 1980 *Annals New York Acad. Sci.* **357** 249

Mandelbrot, B. B., 1982 *The Fractal Geometry of Nature* (Freeman, San Francisco)

Mandelbrot, B. B., 1985 *Physica Scripta* **32**, 257

Mandelbrot, B. B., 1986 in *Fractals in Physics* edited by L. Pietronero and E. Tosatti (Elsevier, Amsterdam) p. 3

Mandelbrot, B. B., 1988 *Fractals and Multifractals: Noise, Turbulence and Galaxies* (Springer, New York)

Meakin, P., 1987 in *Phase Transitions and Critical Phenomena* Vol 12. edited by C. Domb and J. Lebowitz (Academic Press, New York)

Nakanishi, H. and Family, F., 1984 *J. Phys.* **A17**, 427

Nakanishi, H. and Family, F., 1985 *Phys. Rev.* **A32**, 3606

Paladin, G. and Vulpiani, A., 1987 *Phys. Rep.* **156**, 147

Peitgen, H. O. and Richter, P. H., *The Beauty of Fractals* (Springer, Berlin)

Pfeifer, P. and Avnir, D., 1983 *J. Chem. Phys.* **79**, 3558

Pfeifer, P., 1986 in *Fractals in Physics* edited by L. Pietronero and E. Tosatti (Elsevier, Amsterdam) p. 47

Rényi, A., 1970 *Probability Theory* (North-Holland, Amsterdam)

Schaefer, D. W., Martin, J. E., Wiltzius, P. and Cannel, D. S., 1984 in